

PAPER • OPEN ACCESS

## Application of the Schottky diode as a detector of continuous terahertz radiation

To cite this article: A V Badin *et al* 2021 *J. Phys.: Conf. Ser.* **1862** 012012

View the [article online](#) for updates and enhancements.



**IOP | ebooks™**

Bringing together innovative digital publishing with leading authors from the global scientific community.

Start exploring the collection—download the first chapter of every title for free.

# Application of the Schottky diode as a detector of continuous terahertz radiation

**A V Badin, V D Moskalenko and D A Pidotova**

National Research Tomsk State University, 36 Lenin Ave., Tomsk, Russia

E-mail: [thzlab@mail.ru](mailto:thzlab@mail.ru)

**Abstract.** The results of research of the electrophysical and frequency characteristics of the semiconductor structure of a Schottky diode based on gallium arsenide are presented. The diode structure was modelled in the Sentaurus TCAD software package. A comparison of the current-voltage characteristics obtained by mathematical modeling and by experiment are presented. The frequency response in the range of 115-257 GHz is shown. The use of a Schottky diode as a continuous terahertz radiation detector is shown.

## 1. Introduction

Modern devices increasingly require more advanced parts at a low cost. Semiconductor materials are actively involved in the development of electronics, which, due to their unique properties, can be used to create a wide range of power pulse electronics devices, photodetectors, matrix image receivers, and ultra-high frequency (microwave) detectors [1-4]. In particular, in the subterahertz (sub-THz) range (100-300 Hz), the use of Schottky diodes (SD) is promising due to the active development of modern medical technologies, the emergence of contactless security systems, and the development of environmental monitoring devices [5-9].

In comparison with devices based on the p-n junction, the Schottky diode uses a metal-semiconductor junction, which provides it with high speed and low voltage drop. The use of GaAs in diodes is promising due to the large value of band gap and the wide variation of parameters with the introduction of various dopant adding impurities to the material [10-12].

Currently, there is an active implementation of instrument and technological modeling programs for micro- and nanoelectronics. Mathematical modeling allows to analyze the characteristics of devices at the design stage, visualizing physical phenomena and processes in the structure. Synopsys TCAD system (USA) is widely used among manufacturers. The advantage of this modeling system is the possibility of experimental study of samples without their physical implementation. Of the TCAD systems, the Sentaurus TCAD system is the most widely used.

The purpose of this study is to obtain the current-voltage characteristics (CVC) of a Schottky diode on gallium arsenide (GaAs), compare the obtained dependence with the results of mathematical modeling, and test the possibility of using the detector as a receiver of sub-THz radiation.

## 2. Experimental technique

### 2.1. Test sample

For research used an experimental sample of a semiconductor diode with a Schottky barrier (Figure 1).



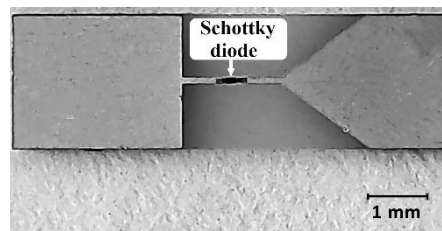


**Figure 1.** Microphotograph of an experimental sample of a Schottky diode.

To create detector structures on a semi-insulating ceramic substrate was deposited n-type gallium arsenide with metal contacts 30 nm thick. Sulfur (S) with an atomic concentration of  $N_d = 10^{18} \text{ cm}^{-3}$  was used as a doping impurity.

### 2.2. Static characteristics of a Schottky diode

To measure the current-voltage characteristics a stationary source Keithley 2410 was used. A negative and positive bias was applied to the diode, and the data was read by an ammeter and voltmeter. The measurement results were automatically recorded as a table on a personal computer (PC).

### 2.3. Frequency characteristics of the Schottky diode

The frequency response was determined using a quasi-optical measuring device [13]. The installation used a backward wave oscillator (BWO) operating in the range of 115-257 GHz, two teflon lenses and a detector placed in the housing. The current increment through the detector was measured using a microammeter. The frequency change step was 5 GHz. To measure the current sensitivity, attenuators of different transmission capacities were additionally installed: 10% and 30% (Figure 2).

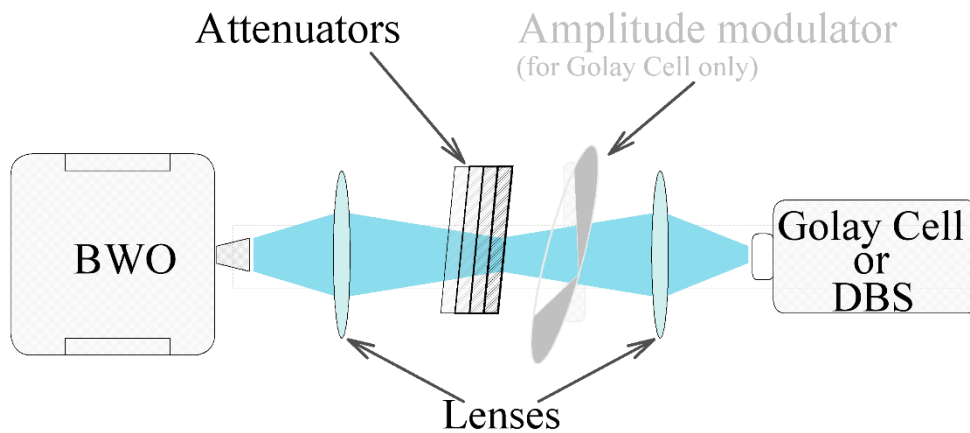


**Figure 2.** Image of a quasi-optical system for studying the current sensitivity of a Sub-THz radiation detector.

At the maximum radiation intensity at a frequency of 249 GHz, CVC was taken for four different cases: when the radiation passed full power, when the radiation was attenuated by 70%, when the radiation was attenuated by 90%, and when there was no radiation. Denoting the passage of radiation without attenuation for 100% of the power corresponding to the average power of the source of 25 mW, the values of the current sensitivity of the SD were obtained.

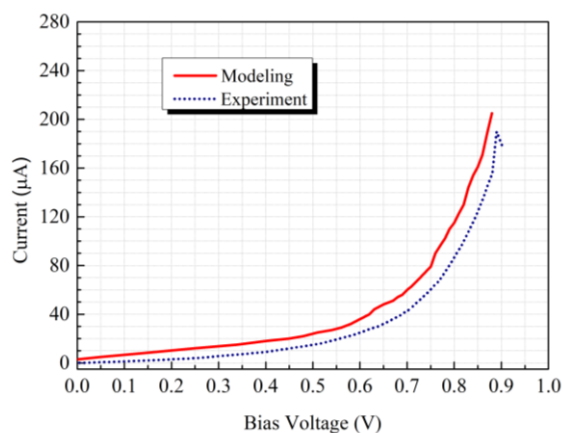
### 2.4. Modeling of current-voltage characteristics in TCAD

In this work, to control the experimental results and tests, the diode was modeled using the Sentaurus TCAD software package. The establishment of a framework began with the geometry of the sample, determining and placement of the contacts. Next step, doping with impurities and applying a grid was performed. The final stage of the work is the construction of the CVC at forward voltage. In the SDevice

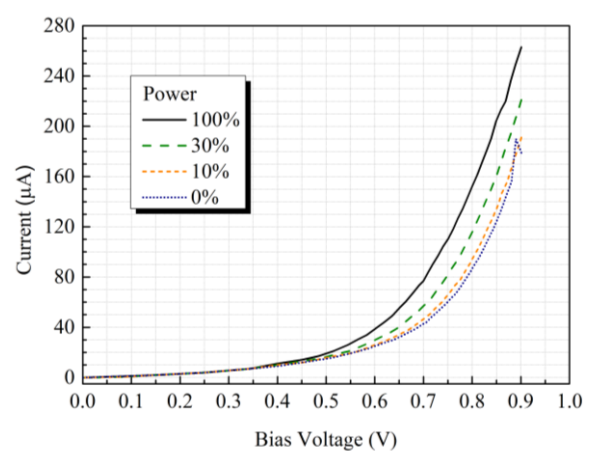
command file specified the initial voltage on the contacts equal to 0 V, the number of iterations equal to 20, the minimum step equal to  $10^{-7}$  V, and the required final value of the voltage on the contact 1V. The simulation takes into account the dependence of the mobility of charge carriers on the concentration and intensity of the electric field. As a result of solving the Poisson equation and the continuity equations for electrons and holes, a set of files containing the current and voltage values in the structure is created. To visualize the results and compare them with the experiment, the data was exported as a table.

### 3. Experimental results

Figure 3 shows a comparison of the current-voltage characteristic of a diode with a Schottky barrier based on *n*-GaAs obtained experimentally and as a result of modeling. The measurements were performed at a forward voltage to determine the value of  $U_b$ . The results of measuring the current-voltage characteristics for different radiation power are shown in Figure 4.

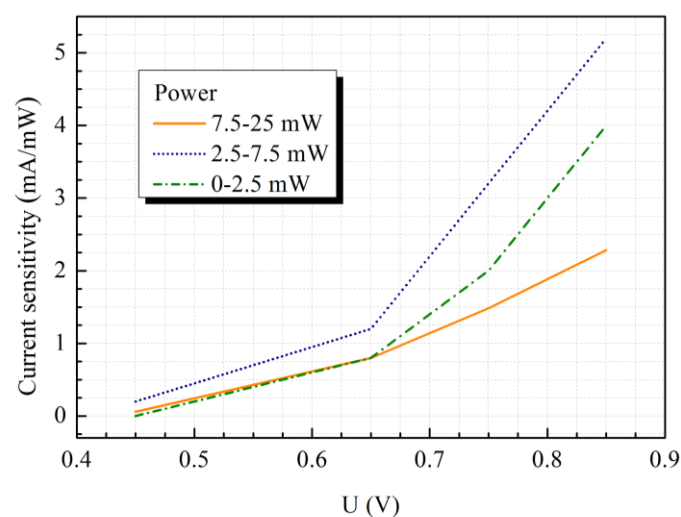


**Figure 3.** CVC of a SD based on *n*-GaAs obtained by experiment and modeling.



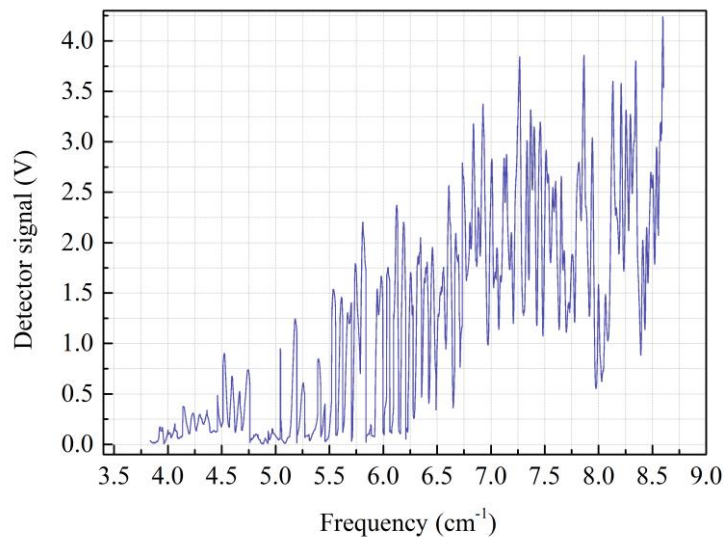
**Figure 4.** CVC of a SD based on *n*-GaAs depending on the relative power of the incident sub-THz radiation.

Figure 5 shows the dependence of the current sensitivity of the diode on the bias voltage.



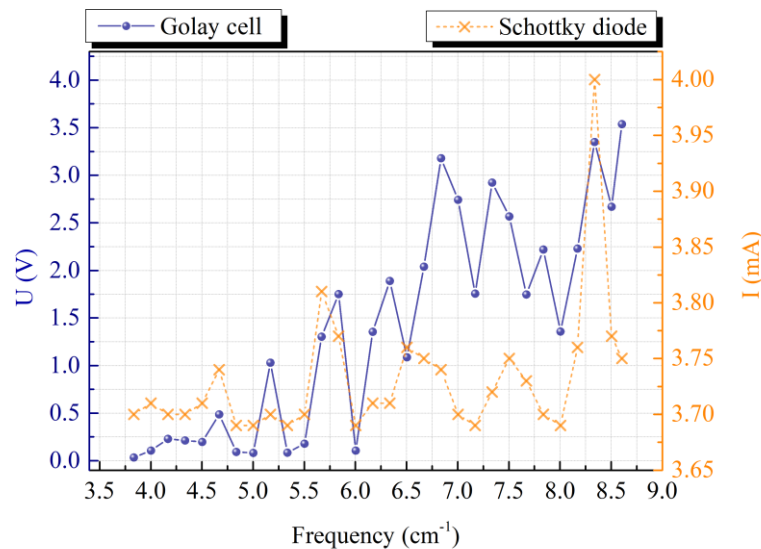
**Figure 5.** Dependence of the current sensitivity of the SD on the bias voltage at a frequency of 249 GHz.

Figure 6 shows the frequency response of the Golay cell in the range of 115-257 Hz. A characteristic feature of BWO based generators is the ripples of the power characteristic, which is manifested on the detector by characteristic peaks and decreases of the signal.



**Figure 6.** The frequency response of the Golay cell in the Sub-THz range.

Similar measurements were made for the Schottky diode. To compare the frequency characteristics, 30 frequency values were selected and the graph shown in Figure 7 was plotted.



**Figure 7.** Frequency response of SD and a Golay cell in the Sub-THz range.

#### 4. Conclusion

Analyzing the CVC of a sample of a diode with a Schottky barrier (Figure 3), obtained experimentally and using simulation, the threshold opening voltage was determined: experimentally  $U_b = 0.706$  V, by modeling  $U_b = 0.625$  V. It should be noted that the simulation sample is a more ideal version of the experimental sample and cannot take into account all the features of the real diode sample. Therefore, although the measured values are close, the difference in the results is present and can be explained by the interaction inside the diode [14], additional defects in the near-surface region of the semiconductor

depending on the methods of metal deposition [15], as well as changes in environmental conditions during experiments [16]. It is assumed that for greater similarity with the results of a natural experiment, it is possible to use several physical models at once, as indicated in [17]. Also, using a linear approximation, the threshold voltage is determined when the radiation passes without attenuation  $U_b = 0.623$  V (Figure 4). The decrease in the threshold voltage in the presence of radiation can be explained, for example, electron-hole scattering (EHS) [18].

Analyzing the current sensitivity graph (Figure 5), it is concluded that an increase in the bias voltage leads to an increase in the increment of current through the Schottky detector, and in the power range of 2.5-7.5 mW, the highest value of the current sensitivity of the diode is observed.

To assess the possibility of replacing the Golay cell with a Schottky diode, a frequency response in the range of 115-257 GHz with an offset of 0.797 V was taken for both detectors and a comparative graph was constructed. The observed correlation (Figure 7) allows us to confirm the assumption that the presented SD can be used as a detector of Sub-THz radiation.

### Acknowledgment

The team of authors is grateful to Gennady F. Kovtunenkov, an employee of the Scientific Research Institute of Semiconductor Devices (SRISD) (Tomsk, Russia) for the samples provided, and Kirill V. Dorozhkin, a Junior researcher at the terahertz research laboratory at the NR TSU for his assistance in conducting the experiment

### References

- [1] Cheng H C *et al* 1990 *Solid State Electron.* **33** 863–867
- [2] Rhoderick E H *et al* 1982 *IEEE Proceedings I Solid State and Electron Devices*, **129** (1), 1
- [3] Kowalczyk S P *et al* 1981 *Appl. Phys. Lett.* **38** 167–9
- [4] Zucca R *et al* 1975 *J. Appl. Phys.* **46** 1396–8
- [5] Ali M *et al* 2018 *25th International Conference on Telecommunications (ICT)* 279–282
- [6] Shur M *et al* 2016 *Micro- and Nanotechnology Sensors, Sys., and Applications VIII* **9836** 1–8
- [7] Ouchi T *et al* 2013 *Terahertz Imaging System for Medical Applications and Related High Efficiency Terahertz Devices* **35** (1), 118–130
- [8] Wang Y *et al* 2020 *Infrared Phys. Technol.* **109** 1–18
- [9] Chen C *et al* 2020 *IEEE Trans. Instrum. Meas.* **69** 5673–5683
- [10] Missoum I *et al* 2016 *Synth. Met.* **214** 76–81
- [11] Ortolani M *et al* 2012 *J. Phys. Conf. Ser.* **359** 1–9
- [12] Biryukov E N *et al* 2018 *Min. Informational Anal. Bull.* **2018** 26–35
- [13] Badin A V *et al* 2017 *International Conference of Young Specialists on Micro/Nanotechnologies and Electron Devices, EDM* 301–304
- [14] Blank T V *et al* 2007 *Semiconductors* **41** 1263–1292
- [15] Barnard W O *et al* 1996 *J. Electron. Mater.* **25** (11) 1695–1702
- [16] Chung S W *et al* 2004 *J. Cryst. Growth* **268** 607–611
- [17] Synopsys 2007 *Sentaurus TM Process User Guide Manual* 778
- [18] Mnatsakanov T T *et al* 2003 *J. Appl. Phys.* **93** 1095–8